J Inorg Organomet Polym (2018) 28:235–250
DOI 10.1007/s10904-017-0706-6

Preparation of Co_3O_4 Nanoparticles via Thermal Decomposition of Three New Supramolecular Structures of Co(II) and (III) Containing 4′-Hydroxy-2,2′:6′,2″-Terpyridine: Crystal Structures and Thermal Analysis Studies

Badri Z. Momeni[1] · Farzaneh Rahimi[1] · Frank Rominger[2]

Received: 20 August 2017 / Accepted: 13 October 2017 / Published online: 20 October 2017
© Springer Science+Business Media, LLC 2017

Abstract Three cobalt(II) and (III) complexes based on the 4′-hydroxy-2,2′:6′,2"-terpyridine (tpyOH) have been synthesized and structurally characterized by X-ray crystallography. The reaction of tpyOH with $CoCl_2{\cdot}6H_2O$ in a mixture of methanol/CH_2Cl_2 resulted in the formation of the new complex $[Co^{II}Cl_2(tpyOH)]$ (**1**). On the other hand, the reaction of $CoCl_2{\cdot}6H_2O$ with tpyOH in a 2:1 or 1:1 mol ratio in methanol under reflux condition affords the new complexes $[Co^{III}(tpyOH)(tpyO)][Co^{II}Cl_4]{\cdot}H_2O$ (**2**) and $[Co^{III}Cl_2(H_2O)(tpyO)]{\cdot}H_2O$ (**3**), respectively. Moreover, the treatment of a methanolic solution of $CoCl_2{\cdot}6H_2O$ with tpyOH in a branched tube at 60 °C resulted in the formation of three quality crystals of the complexes **1** and **2** as the major products as well as the complex **3** as a minor product. The crystal structure of $[CoCl_2(tpyOH)]$ (**1**) reveals that the cobalt(II) is penta-coordinated by two Cl^- and three nitrogen atoms of tpyOH in a distorted square pyramidal geometry. The complex $[Co^{III}(tpyOH)(tpyO)][Co^{II}Cl_4]{\cdot}H_2O$ (**2**) is described as a highly distorted octahedral geometry $[CoN_6]$ while the X-ray crystal structure of the complex $[Co^{III}Cl_2(H_2O)(tpyO)]{\cdot}H_2O$ (**3**) shows that cobalt(III) is hexa-coordinated in a slightly distorted octahedral geometry $CoCl_2N_3O$. Several strong noncovalent interactions are present in the crystal structure of **1**–**3**. The hydrogen bonding in **1** involves the OH···Cl bridges while there is a hydrogen bonding between tpyO and tpyOH of the next molecule in **2** and hydrogen bridges and π–π interactions for **3**, connecting molecules and ions in the crystalline **1**–**3** to form supramolecular networks. The thermal stabilities of the cobalt complexes reveal that the loss of free terpyridine ligand could not be observed in low temperatures. The hexagonal and spherical Co_3O_4 nanoparticles (NPCs) were prepared by direct calcination of complexes **1**–**3** at 600 °C in air. The nanostructures of the products were characterized by IR, powder X-ray diffraction, field emission scanning electron microscopy and energy-dispersive X-ray spectroscopy which show the purity of the resulting Co_3O_4 NPCs. The average particle size using Scherrer's equation is calculated to be about 32–35 nm.

Keywords Cobalt · Terpyridine · Crystal structure · Co_3O_4 NPCs · Thermal analysis

1 Introduction

Transition metal complexes of 2,2′:6′,2″-terpyridine ligand have been studied extensively since the ligand was first reported at 1932 by Morgan and Burstall [1]. A vast number of methods are known for the preparation of substituted terpyridines. Most of these methods are based on the 2-acetyl pyridines and aryl aldehydes [2–5]. 4-Substituted-2,6-diacetylpyridines have been used to prepare 2,2′:6′,2"-terpyridine functionalized at $C_{4'}$ and containing substituents at C_4, C_5 and C_6 of both terminal pyridines [6]. Terpyridine complexes of transition metals such as cobalt have attracted considerable interest due to their applications in medicinal chemistry, catalysis, crystal engineering and supramolecular chemistry [7–12]. The use of ligands with multiple-metal binding domains is of particular interest, since they can be linked by a metal-containing moiety instead of an organic group, such as 4′-pyridyl, carboxylic acid, hydroxy or 4′-carboxyphenyl-2,2′:6′,2″-terpyridines

✉ Badri Z. Momeni
momeni@kntu.ac.ir

[1] Faculty of Chemistry, K.N. Toosi University of Technology, P.O. Box 16315-1618, Tehran 15418, Iran

[2] Organisch-Chemisches Institut, Universität Heidelberg, 69120 Heidelberg, Germany

[13–20]. 4′-Hydroxy-2,2′:6′,2″-terpyridine (tpyOH) is a ubiquitous ligand and a variety of stable transition metal complexes of tpyOH has been reported which are useful in the design and construction of multi-pyridyl complexes and applications such as catalysis and supramolecular chemistry. TpyOH can, and often do, take advantage of its potential to act as a tridentate ligand in a symmetrical binding mode. However, it has potential to chelate metals or can further bridge metal sites through the deprotonation of the hydroxy group, resulting in the formation of 1D, 2D or 3D-coordination polymers [20–26]. For example, the Cu(II) center in $[Cu(tpyOH)](ClO_4)_2$ has a pseudo-square planar geometry via three terpyridyl N atoms and an oxygen atom from a coordinated water molecule [26]. Interestingly, in the case of $[Co(4\text{-terpyridone})_2]X_2{\cdot}nH_2O$ ($X = SO_4^{2-}$, Cl^-, ClO_4^-), the cobalt center is hexa-coordinated in a *mer*-fashion of a tetragonally distorted compressed $[CoN_6]$ compressed octahedral [27]. A novel spin crossover phenomenon has been observed in the bis-terpyridine complexes of cobalt(II) and cobalt(III) [27–30]. The complex stability constants of 1:1 solution of $MnCl_2$: tpyOH has shown the presence of a mixture of 1:1 and 1:2 complex species in an aqueous alkaline solution. The presence of π-donor substituent of hydroxy or amine groups in 4′-position of terpyridine has increased the catalytic activity of $MnCl_2$–tpyOH system to activate the hydrogen peroxide and oxidation of Morine and Trolox C bleach [31].

Co_3O_4 with the normal spinel crystal structure is an important metal oxide which is anti-ferromagnetic p-type semi-conductor with the excellent properties. Co_3O_4 nanoparticles show biological toxicity as well as interesting magnetic and optical properties which are attractive in device applications [32–35]. Recently, the preparation of Co_3O_4 nanoparticles has been a target of many material chemists and there are various synthesis methods, such as chemical spray pyrolysis [36], sol–gel [37], solvothermal [38] and hydrothermal [39] methods. It has been found that metal coordination complexes can be suitable precursors for the preparation of metal oxide nanoparticles. For example, transition metal complexes of Schiff base, diimine, pyridine carboxylic acid, terpyridine have been used for the preparation of nanoparticle structures [23, 39–44]. It has been found that the morphology of Co_3O_4 nanoparticles influences the biological toxicity of these nanostructures [32].

This paper reports the preparation of the three hydroxy-terpyridine complexes of Co(II) and Co(III) containing tpyOH via a facile synthesis. The crystal structures of the three new complexes of cobalt containing different structural features are discussed. Thermal behavior of the cobalt complexes has also been studied. The resulting complexes have been used as precursors to prepare the Co_3O_4 nanoparticles (Co_3O_4 NPs) with different sizes and morphologies. The structures and morphologies of the resulting nanoparticles were characterized by IR, XRD, FESEM and EDX.

2 Experimental

2.1 General Remarks

Elemental analyses were performed by Thermo Finnigan Flash Ea 111 elemental analyzer. IR spectra in the $4000-400\ cm^{-1}$ were recorded on KBr pellets using ABB Bomem Model FTLA200-100 spectrophotometer. Each spectrum was recorded with a spectral resolution of $4\ cm^{-1}$ and scan's numbers of 10 using a deuterated-triglycine sulfate (DTGS) detector. TGA data was collected by NETZSCH TG 209 F1 Iris at a heating rate of 10 K min^{-1} under an N_2 atmosphere. The XRD patterns were recorded in the 2θ range of 10°–80° using a PHILIPS PW1730 by CuKα radiation, kα = 1.5406 Å. Field emission scanning electron microscopy (FESEM) images were obtained using a TESCAN MIRA II (Scanning Electron Microscope) device, operating at an accelerating voltage 10 kV, equipped with energy dispersive spectroscopy (EDX). 4′-Hydroxy-2,2′:6′,2″-terpyridine (tpyOH) was prepared according to the literature [45].

2.2 Synthesis of $[Co(tpyOH)Cl_2]$ (1)

A solution of $CoCl_2{\cdot}6H_2O$ (24 mg, 0.10 mmol) in methanol (2 mL) was added to a solution of tpyOH (25 mg, 0.10 mmol) in CH_2Cl_2 (2 mL) at room temperature. The color of the reaction mixture turned to brown. The mixture was then stirred for 2 h after which the brown solid was isolated by filtration and washed with diethyl ether. Yield: 92%; m.p. 364–366 °C (dec.). Anal. Calc. for $C_{15}H_{11}Cl_2CoN_3O$ (%): C, 47.52; H, 2.92; N, 11.08. Found; C, 48.01; H, 2.79; N, 11.06. IR data (KBr, cm^{-1}): 3436 (O–H), 3063 (=C–H), 2559, 1612 (C=N, C=C), 1472, 1371, 1228, 1163, 1027 (O–H, C–O). TGA: calc. by formula $C_{15}H_{11}Cl_2CoN_3O{\cdot}H_2O$: 1 H_2O% = 4.54, 2Cl% = 18.70, 2.5 pyridine% = 64.16. Determined: 1 H_2O% = 3.74, 2Cl% = 19.17, 2.5 pyridine% = 66.17. Green crystals of **1** were obtained from a methanolic solution of **1**.

2.3 Synthesis of $[Co(tpyOH)(tpyO)][CoCl_4]{\cdot}H_2O$ (2)

To a solution of $CoCl_2.\ 6H_2O$ (24 mg, 0.10 mmol) in methanol (10 mL) was added a solution of tpyOH (50 mg, 0.20 mmol) in methanol (10 mL) which was refluxed at 60 °C for 2 h. The solvent was then removed at reduced pressure and the residue was precipitated using diethyl ether to give a brown solid. Yield: 80%; m.p. 323–325 °C (dec.). Anal. Calc. for $C_{30}H_{21}Cl_4Co_2N_6O_2{\cdot}H_2O$ (%): C, 46.48;

H, 2.99; N, 10.84. Found; C, 46.74; H, 3.01; N, 10.95. IR data (KBr, cm^{-1}): 3753, 3395 (O–H), 3031 (=C–H), 1611, 1532 (C=C, C=N), 1469, 1373, 1232, 1097, 1026 (O–H, C–O). TGA: calc. by formula TGA: calc. by formula $C_{30}H_{21}Cl_4Co_2N_6O_2{\cdot}4\ H_2O$:3$H_2O$% = 6.52, 1Cl and 1$H_2O$% = 6.90, 3Cl% = 14.74, 2py and 1OH. Determined: 3H_2O% = 7.29, 1Cl and 1H_2O% = 6.27, 3 Cl% = 16.39, 2py and 1OH = 29.50.

2.4 Synthesis of $[CoCl_2(H_2O)(tpyO)]{\cdot}H_2O$ (3)

Similarly, the complex **3** was synthesized following the same procedure as the preparation of **2** using tpyOH (25 mg, 0.10 mmol) and $CoCl_2{\cdot}6H_2O$ (24 mg, 0.10 mmol) in methanol (5 mL) to give a green solid. Yield: 85%; m.p. 368–370 °C (dec.). Anal. Calc. for $C_{15}H_{12}Cl_2CoN_3O_2$ (%): C, 45.48; H, 3.05; N, 10.61. Found; C, 45.25; H, 2.93; N, 10.58. IR data (KBr, cm^{-1}): 3254 (O–H), 3029 (=C–H), 1621 (C=O), 1566, 1478, 1363 (C–N), 1224, 1168, 1026 (C–OH), 868, 799 (=C–H), 751, 725, 627, 569. TGA: calc. by formula $C_{15}H_{15}Cl_2CoN_3O_2$: H_2O% = 4.52, 0.5Cl% = 4.65, tpyO and Cl% = 78.08. Determined: H_2O% = 5.86, 0.5Cl% = 3.36, tpyO and Cl% = 78.68.

2.5 Preparation and Crystal Growth of [Co(tpyOH)Cl_2] (1), $[Co(tpyOH)(tpyO)][CoCl_4]{\cdot}H_2O$ (2) and $[CoCl_2(H_2O)(tpyO)]{\cdot}H_2O$ (3)

Alternatively, complexes **1–3** were prepared by branched tube methods as follows: tpyOH (50 mg, 0.20 mmol) was placed in the side arm of the branched tube and $CoCl_2{\cdot}6H_2O$ (54 mg, 0.20 mmol) was placed in the main arm. Methanol (10 mL) was carefully added to fill the tube. The tube was then sealed and the main arm was immersed in an oil bath at 60 °C while the side arm remained at room temperature. After one week, three suitable single crystals of **1, 2** and **3** were formed. These crystals could be realized by their colors; the green crystals of **1** were formed in the arm of branched tube where it was placed in the ambient temperature. The brown block type crystals of **2** were found in the bottom of the tube where it was immersed in the bath at 60 °C and the small amounts of violet plate crystals of **3** were formed in the top of the tube. Yield for **1**: 45%. Yield for **2**: 42%.

2.6 Preparation of Co_3O_4 Nanoparticles Using 1–3 as Precursors

The complexes of $[Co(tpyOH)Cl_2]$ (**1**), $[Co(tpyOH)(tpyO)][CoCl_4]{\cdot}H_2O$ (**2**) and $[CoCl_2(H_2O)(tpyO)]{\cdot}H_2O$ (**3**) were heated at a rate of 20 °C /min in a furnace muffle at 600 °C in air. After 2 h, they were allowed to cool to room temperature to form black Co_3O_4 nanoparticles.

2.7 Crystal Structure Determination and Refinement

Green crystal (polyhedron) of (**1**), brown crystal (block) of (**2**) and violet crystal (plate) of (**3**) with CCD area detector, covering the asymmetric unit in reciprocal space were corrected for Lorentz and polarization effects. An empirical absorption correction was applied using SADABS [46] based on the Laue symmetry of the reciprocal space. The structures refined against F^2 with a Full-matrix least-squares algorithm using the SHELXL-2014/7 (Sheldrick, 2014) software [47]. The hydrogen atoms were treated using appropriate riding models, except H1 of the hydroxy group for (**1**), which was refined isotropically and those at the oxygen atoms of (**2**) which were either refined isotropically (at O_2) or not modeled at all (at the crystal water molecule O_3) and those assumed at the oxygen atoms of (**3**) that could not be located and have been not included into the model. A summary of crystal data, experimental details, and refinement results is given in Table 1.

3 Results and Discussion

3.1 Synthesis and Structures of the Cobalt Complexes

The reaction of $CoCl_2{\cdot}6H_2O$ with tpyOH in a molar ratio of 1:1 in CH_2Cl_2/MeOH solvent afforded the mononuclear complex of $[Co^{II}Cl_2(tpyOH)]$ (**1**) as shown in Scheme 1. The product was characterized by IR, elemental analysis and X-ray structure determination.

The crystal structure of $[CoCl_2(tpyOH)]$ (**1**) shows that Co^{2+} is penta-coordinated by two Cl^- and three nitrogen atoms of tpyOH as shown in Fig. 1. The coordination geometry of cobalt can be best described as a distorted square pyramid. The basal plane is composed of three nitrogen atoms from tpyOH and one of the two chlorides. Another chloride occupies the apical position. The three pyridine rings are almost in the same plane. The Co1–N1 bond distance involving the central nitrogen atom (2.0426 Å) is shorter than those concerning the terminal nitrogen atoms (Co–N2 = 2.145(2) Å and Co–N3 = 2.167(2) Å) as a result of chelating ligand constrain [20]. The dihedral angles between the middle pyridine ring and each of the other edge pyridine is very small; 7.33° for the N2 containing pyridine and 9.96° for the N3 containing pyridine ring. The interplanar spacing of successive centroid–centroid pyridines of the parallel terpyridine moieties is about 4.58 Å. The hydroxy is slightly tilted from the parallel terpyridine planes by the angle of 2.65°. The only hydrogen bonding is a OH···Cl bridge (Table 2), building a supramolecular assembly in the solid state as shown in Fig. 2.

The reaction of $CoCl_2{\cdot}6H_2O$ with tpyOH in a molar ratio of 1:2 or 1:1 in methanol under reflux condition resulted in

Table 1 Crystal data and structure refinement for $[CoCl_2(tpyOH)]$ (**1**), $[Co(tpyOH)(tpyO)][CoCl_4]\cdot H_2O$ (**2**) and $[CoCl_2(H_2O)(tpyOH)]\cdot H_2O$ (**3**)

	1	2	**3**
Empirical formula	$C_{15}H_{11}Cl_2CoN_3O$	$C_{30}H_{21}Cl_4Co_2N_6O_2\cdot H_2O$	$C_{15}H_{12}Cl_2CoN_3O_2\cdot H_2O$
Formula weight	379.10	773.19	414.13
Temperature (K)	200 (2)	200 (2)	200 (2)
Wavelength (Å)	0.71073	0.71073	0.71073
Crystal system	Triclinic	Monoclinic	Monoclinic
Space group	$P\bar{1}$	$P2_1/c$	$P2_1/c$
Z	2	4	4
a (Å)	8.0825 (3)	8.8594 (17)	18.771 (11)
b (Å)	8.6202 (4)	23.391 (4)	13.170 (8)
c (Å)	11.3341 (5)	15.236 (3)	6.617 (4)
α (°)	105.4509 (10)	90	90
β (°)	95.5954 (10)	98.357 (3)	90.219 (11)
γ (°)	105.0823 (9)	90	90
V ($Å^3$)	723.02 (5)	3123.7 (10)	1614.8 (17)
D_{calc} (g/cm^3)	1.74	1.64	1.71
μ (mm^{-1})	1.56	1.45	1.41
Crystal shape	Polyhedron	Block	Plate
Crystal size	0.090 × 0.080 × 0.070	0.081 × 0.057 × 0.040	0.077 × 0.077 × 0.016
Crystal colour	Green	Brown	Violate
θ range (°)	1.9–25.1	1.6–23.6	1.1–25
Index ranges	$-9 \le h \le 9$	$-9 \le h \le 9$	$-22 \le h \le 22$
	$-10 \le k \le 10$	$-26 \le k \le 26$	$-15 \le k \le 15$
	$-13 \le l \le 13$	$-17 \le l \le 17$	$-7 \le l \le 7$
Reflections collected	15,886	32,338	14,895
Independent reflections	2579 ($R_{int} = 0.0354$)	4686 ($R_{int} = 0.1474$)	2890 ($R_{int} = 0.0749$)
Observed reflections	2254 (I > 2 σ (I))	3110 (I > 2 σ (I))	2532 (I > 2 σ (I))
Absorption correction	Semi-empirical from equivalents	Semi-empirical from equivalents	Semi-empirical from equivalents
Max. and min. transmission	0.91 and 0.84	0.95 and 0.75	0.97 and 0.83
Refinement method	Full-matrix least-squares on F^2	Full-matrix least-squares on F^2	Full-matrix least-squares on F^2
Data/restraints/parameters	2579/210/203	4686/0/410	2890/228/218
GOF on F^2	1.10	1.07	1.03
Final R indices [I > 2σ(I)]	$R_1 = 0.028$	$R_1 = 0.061$	$R_1 = 0.109$
	$wR_2 = 0.064$	$wR_2 = 0.115$	$wR_2 = 0.278$
Largest diff. peak and hole ($eÅ^{-3}$)	0.34 and −0.26	0.59 and −0.0.70	2.23 and −1.72

Scheme 1 Reaction of tpyOH with $CoCl_2\cdot 6H_2O$

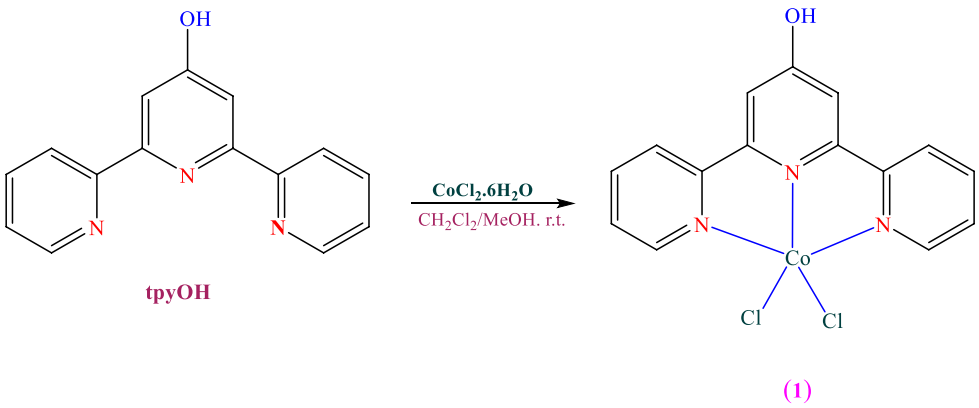

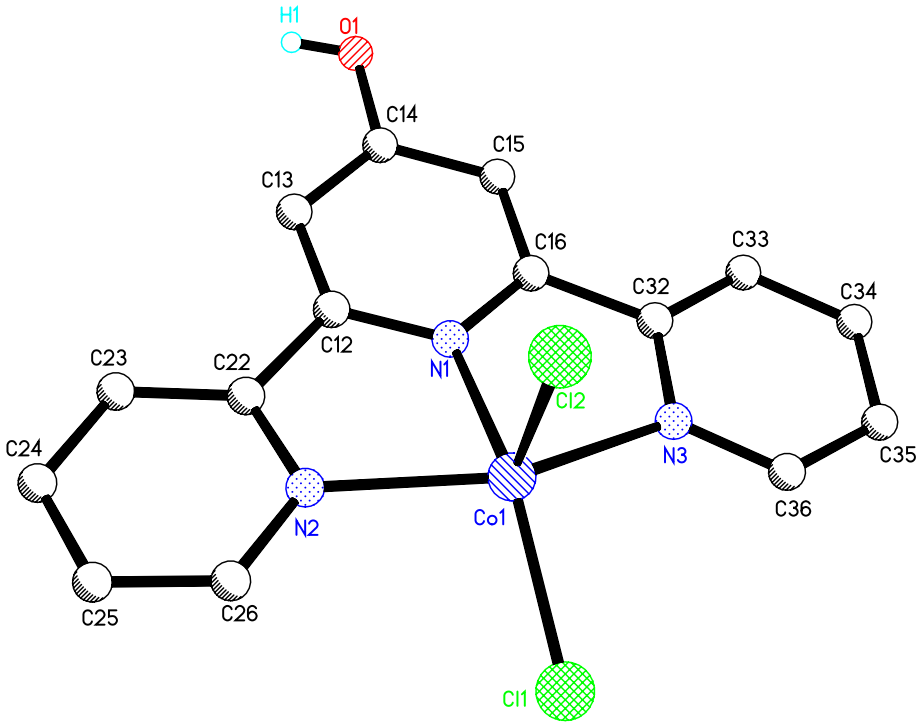

Fig. 1 ORTEP diagram for $[CoCl_2(tpyOH)]$ (**1**). Selected bond distances (Å) and angles (°): Co1–N1 2.0426(19), Co1–N2 2.145(2), Co1–N3 2.167(2), Co1–Cl1 2.2720(7), Co1–Cl2 2.3458(7), N1–Co1–N2 75.90(7), N1–Co1–N3 75.91(7), N2–Co1–N3 149.46(8), N1–Co1–Cl1 149.57(6), N2–Co1–Cl1 100.26(6), N3–Co1–Cl1 98.07(5), N1–Co1–Cl2 101.76(6), N2–Co1–Cl2 98.86(6), N3–Co1–Cl2 98.14(6), Cl1–Co1–Cl2 108.63(3), C12–N1–C16 119.9(2), C12–N1–Co1 120.07(15), C16–N1–Co1 119.43(16),C26–N2–Co1 125.83(17), C22–N2–Co1 115.63(15), C36–N3–Co1 127.26(16), C32–N3–Co1 114.56(15)

Table 2 Hydrogen-bond geometry (A, °) for complexes **1** and **2**

Complex	D–H···A	D–H	H···A	D···A	D–H···A
1	O1–H1···Cl2	0.76	2.28	3.03	168
2	O2–H2···O1	1.01	1.45	2.43	165

the formation of the bis-terpyridine complex $[Co^{III}(tpyOH)(tpyO)][Co^{II}Cl_4]\cdot H_2O$ (**2**) or mono-terpyridine complex $[Co^{III}Cl_2(H_2O)(tpyO)]\cdot H_2O$ (**3**), respectively, as shown in Scheme 2.

Interestingly, using amounts of $CoCl_2\cdot 6H_2O$ in a molar ratio of $CoCl_2$ tpyOH/1:1 in methanol solution at 60 °C in a branched tube, the three complexes of $[Co^{II}Cl_2(tpyOH)]$ (**1**) and $[Co^{III}(tpyOH)(tpyO)][Co^{II}Cl_4]\cdot H_2O$ (**2**) (major products) and $[Co^{III}Cl_2(H_2O)(tpyO)]\cdot H_2O$ (**3**) (minor product) were also prepared as shown in Scheme 3. The above reactions show the effect of the temperature, organic ligands, reaction solvent and conditions on the structural features of the terpyridine complexes.

Crystal structure of $[Co^{III}(tpyOH)(tpyO)][Co^{II}Cl_4]\cdot H_2O$ (**2**) displays that terpyridines exist as a mixture of the ligands

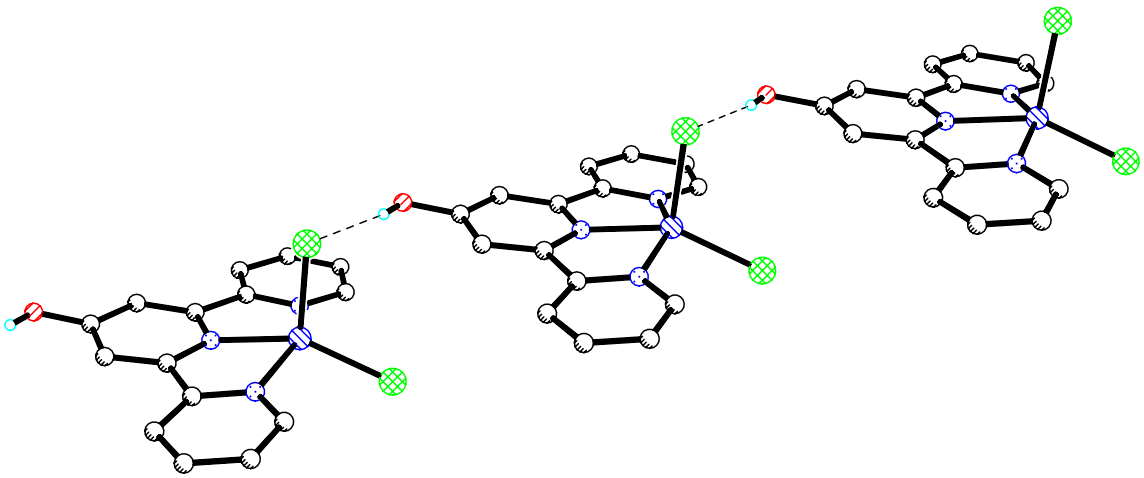

Fig. 2 Crystal packing of$[CoCl_2(tpyOH)]$ (**1**) in b axis

Scheme 2 Preparation of terpyridine complexes **2**–**3**

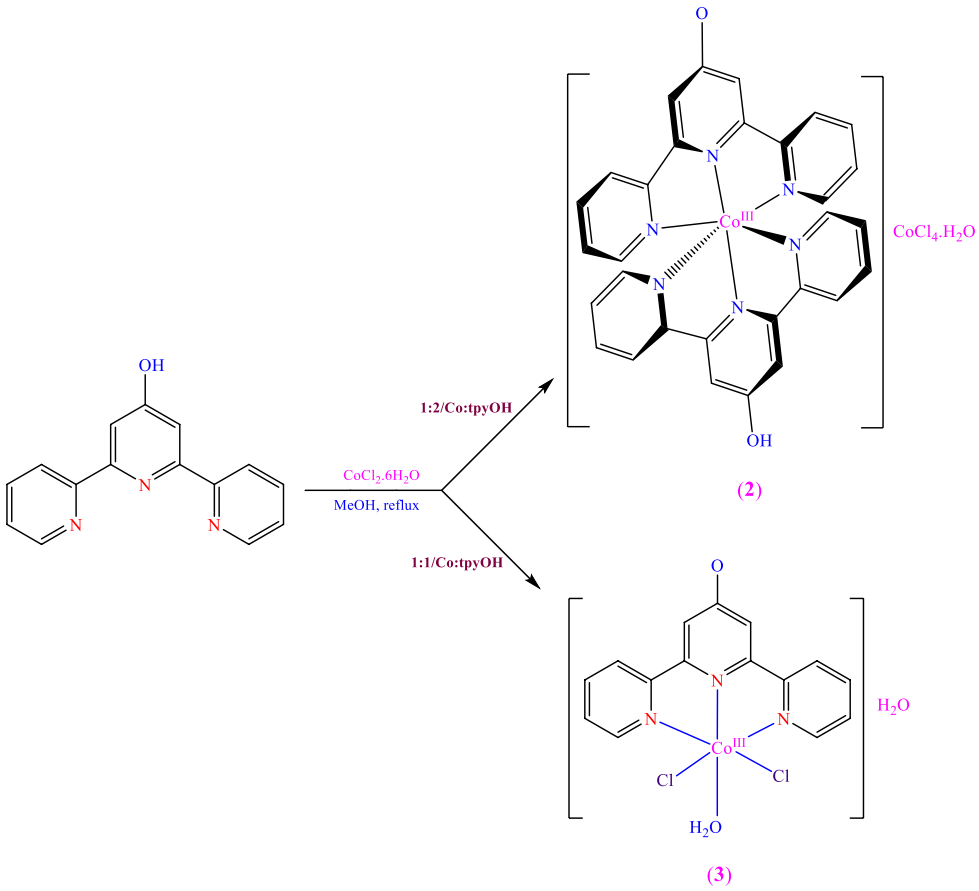

of tpyOH and tpyO, confirming that the cation is indeed $[Co^{III}(tpyOH)(tpyO)]^{2+}$. The cobalt(III) coordination environment is best described a hexa-coordinated CoN_6 environment with a *mer*-octahedral geometry, with coordination to six nitrogen atoms of tpyO and tpyOH (Fig. 3). The structure of complex **2** is composed of discrete $[Co(tpyOH)(tpyO)]^{2+}$ cation, $CoCl_4^{2-}$ anion and a H_2O molecule. The tpyOH and $tpyO^-$ are tridentate ligands and linked to the Co(III) atom via three N atoms. The tridentate N_3–*tpyO* and N_3–tpyOH ligands coordinate in a *mer*-fashion giving a distorted CoN_6 compressed octahedron. The Co–N distances fall into two ranges; those involving the central pyridine rings are almost the same (Co–N1 = 1.856(5) Å and Co1–N4 = 1.851(5) Å); however, those involving the outer four pyridines are little longer (Co1–N6 = 1.923(6), Co1–N3 = 1.945(5), Co1–N5 = 1.948(6), Co1–N2 = 1.952(6) Å). In each terpyridine, the central Co–N bond distances are shorter than those concerning terminal bond distances. The inability of the terpyridine ligand to form a regular octahedral complex is also reflected in the N–Co–N angles of each terpyridine ligand. They are reduced from the ideal value of 180°, particularly the angles N6–Co1–N5 = 164.1° and N3–Co1–N2 = 164.4°. The terpyridine ligands are twisted respect to each other at 88.41° which are almost perpendicular to each other. The outer pyridine rings of each terpyridine unit are also twisted relative to the central rings (4.8°–6.9°). The packing diagram of **2** reveals the presence of 4′-OH···4′-O hydrogen bonding (OH···O distance of 1.45 Å) in the crystal structure, as two oxygens share one common hydrogen atom as shown in Fig. 4 (Table 2). The $CoCl_4^{2-}$ forms a slightly distorted tetrahedral geometry as revealed by Cl–Co–Cl angles which deviate from tetrahedral geometry (112.58(8)°). In addition, a water solvent molecule was found in the crystal, although the H atoms belonging to water molecules were not found. Chains in the adjacent sheets are arranged as shown in Fig. 5 with face-to-face and edge-to-face stacking between terpyridine domains in which alternative terpyridines are twisted to each other at 9.27° to form a supramolecular network.

We could not be successful in the full characterization of $[CoCl_2(H_2O)(tpyO)]\cdot H_2O$ (**3**) due to the presence of the light atoms of hydrogen on tpyOH and H_2O (Fig. 6). However, there are several considerations that can be made to shed light on the hydrogen location. The bond length of O1–C14 is 1.24 Å, rather short and thus more of the tpyO

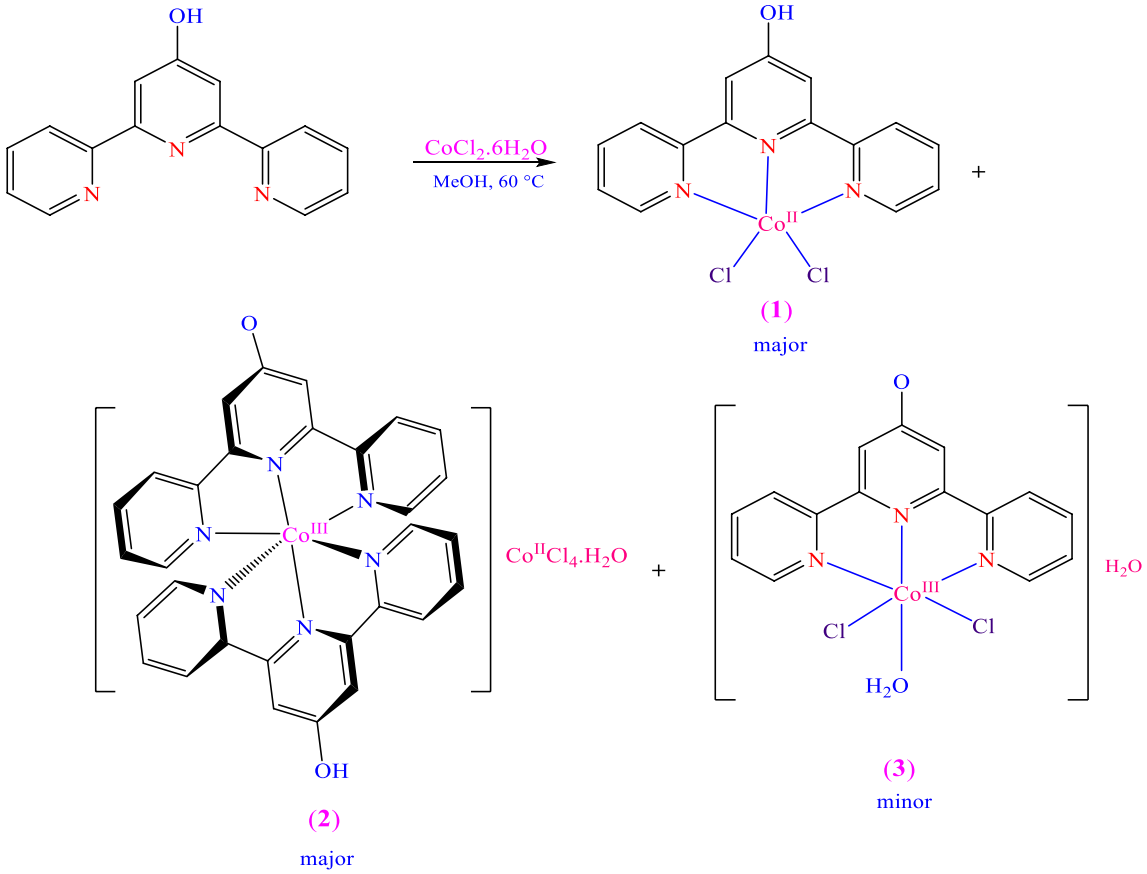

Scheme 3 Preparation of terpyridine complexes **1–3** in a branched tube

than tpyOH. The hydrogen bond of solvent crystal water is in a distance of 2.79 Å which is more typical for $H_2O\cdots O–C$ than for $H_2O\cdots HO–C$. On the other hand, the coordination distance Co1–O2 of 2.22 Å is typical for Co–H_2O *trans* to Cl, a shorter bond distance would be expected for OH. Notably, a search of the Cambridge Structural Database shows no *trans* Cl–Co–OH bond distance at all. Therefore, considering the above distances, we may say that it looks more like tpyO and Co–H_2O than the other way round, but the point is that we can't be sure from the diffraction analysis. The Co–N bond distances show a rather different behavior. The terminal pyridines of the tpyO are strongly bound (Co1–N1 = 2.250(10), Co1–N1 = 2.103(11), Co1–N3 = 2.094(11) Å). Neighboring monomer units along the b-chain are tilted by 5.81° from one another while the second unit is tilted by 6.22° in a face-to-face stacking. The dihedral angles between the middle pyridine ring and each of the other outer pyridine are 2.75° for the N2 containing pyridine and 1.54° for the N3 containing pyridine ring. The H atoms belonging to the water molecule and aqua ligand were not found. The water molecule (oxygen atom) position is fully occupied and there is not positional disorder. The O3···O1 distance (D···A = 2.792 Å) points that one of the H atoms of water (O3) molecule should be located along the O3···O1 with O3–H distance of 0.82 Å (Fig. 7). Therefore, the coordinate of H (X, Y, Z) can be calculated and introduced to the ins file and refined. Next, the other H atom should be located from geometrical correlation (also with O3–H distance of 0.82 Å and the H–O3–H angle of about 105°. The crystal structure of **3** is stabilized by the strong hydrogen bonding networks involving two solvent crystal waters as well as the hydrogen bonding between solvent crystal water and the oxygen from $tpyO^-$ (Fig. 8). In addition, there are two hydrogen bonding interactions between each of the aqua ligand and two chlorides from two neighboring molecules. The interplanar distances of the successive nitrogen terpyridine moieties suggest possible π–π interactions in complex **3** (Fig. 9). Analysis of short ring interactions indicate the presence of π–π interactions of Cg(2)···Cg(2), 3.823(8) Å and Cg(3) Cg(3), 3.784(8) Å (where Cg(4):N(2)–C(22)–C(23)–C(24)–C(25)–C(26) and Cg(5):N(3)–C(32)–C(33)–C(34)–C(35)–C(36)).

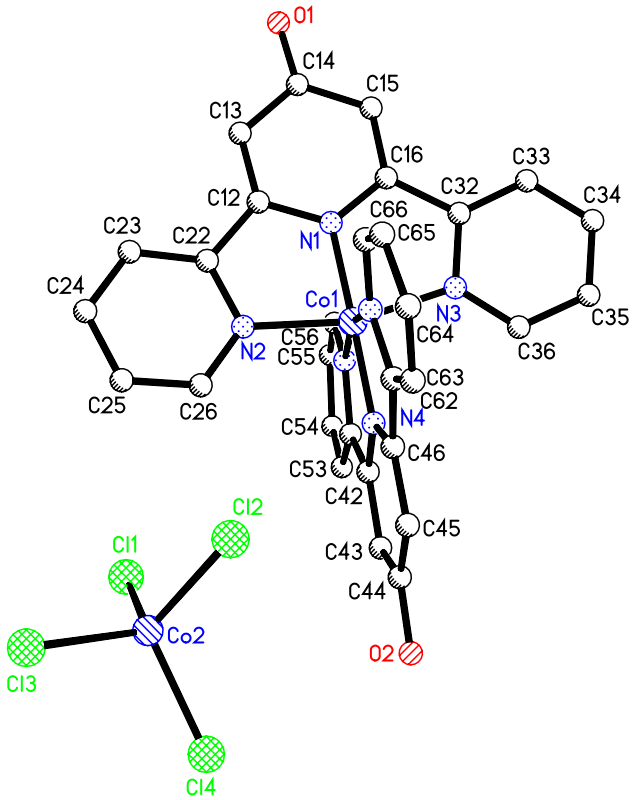

Fig. 3 ORTEP diagram for [Co(tpyOH)(tpyO)][$CoCl_4$]·H_2O (**2**). Selected bond distances (Å) and angles (°): Co1–N4 1.851(5), Co1–N1 1.856(5), Co1–N6 1.923(6), Co1–N3 1.945(5), Co1–N5 1.948(6),Co1–N2 1.952(6), Co2–Cl4 2.260(2), Co2–Cl1 2.273(2), Co2–Cl2 2.282(2), Co2–Cl3 2.298(2), N4–Co1–N1 178.1(2), N4–Co1–N6 82.3(2), N1–Co1–N6 99.5(2), N4–Co1–N3 98.6(2), N1–Co1–N3 82.2(2), N6–Co1–N3 89.2(2), N4–Co1–N5 81.8(2), N1–Co1–N5 96.4(2), N6–Co1–N5 164.1(2), N3–Co1–N5 92.0(2), N4–Co1–N2 96.8(2), N1–Co1–N2 82.5(2), N6–Co1–N2 90.7(2), N3–Co1–N2 164.4(2), N5–Co1–N2 92.4(2), Cl4–Co2–Cl1 112.58(8), Cl4–Co2–Cl2 110.94(9), Cl1–Co2–Cl2 106.79(9), Cl4–Co2–Cl3 106.89(9), Cl1–Co2–Cl3 112.27(8), Cl2–Co2–Cl3 107.29(9)

In summary, 4′-hydroxy-2,2′:6′,2"-terpyridine is described in which 4′-hydroxy plays an important role in the structure determination [20]. The role of metal center, anion, solvent and temperature should be considered in crystal engineering design.

4 Preparation and Characterization of Co_3O_4 Nanoparticles

The black Co_3O_4 nanoparticles were obtained from thermal treatment of cobalt complexes **1**–**3** at 600 °C for 2 h. The IR spectrum of Co_3O_4 contains two strong absorption bands at 668 and 586 cm^{-1}, which confirm the spinel structure of Co_3O_4 (Fig. 10). The peak at 668 cm^{-1} is attributed to the vibration mode of Co–O, in which Co^{+2} in the tetrahedrally coordinated. The band at 586 cm^{-1} is assigned to the Co–O bond due to the octahedrally coordinated of Co^{+3} [42].

The XRD patterns of the obtained Co_3O_4 NPCs were also shown in Fig. 11. The nanoparticles sizes of the Co_3O_4 NPCs (d), were calculated from the diffraction peaks due to the Scherrer formula as shown in Eq. (1) [48].

$$d = \frac{\kappa\lambda}{\beta \cos\theta} \tag{1}$$

where κ is a constant (ca. 0.9); λ is the X-ray wavelength used in XRD (1.5418 Å); Θ the Bragg angle and β is the pure diffraction broadening of a peak at half-height. The average diameter of Co_3O_4 NPs is 35.11, 32.25 and 33.17 nm for prepared Co_3O_4 nanoparticles from complexes **1**, **2** and **3**, respectively. The diffraction peaks of prepared NPCs are similar to those of pure Co_3O_4 with normal spinel structure. On the other hand, the quantitative results of EDX analysis display the presence of the cobalt and oxygen (Fig. 12). The results show the same pattern for all three products resulting from terpyridine complexes **1**–**3** which confirm

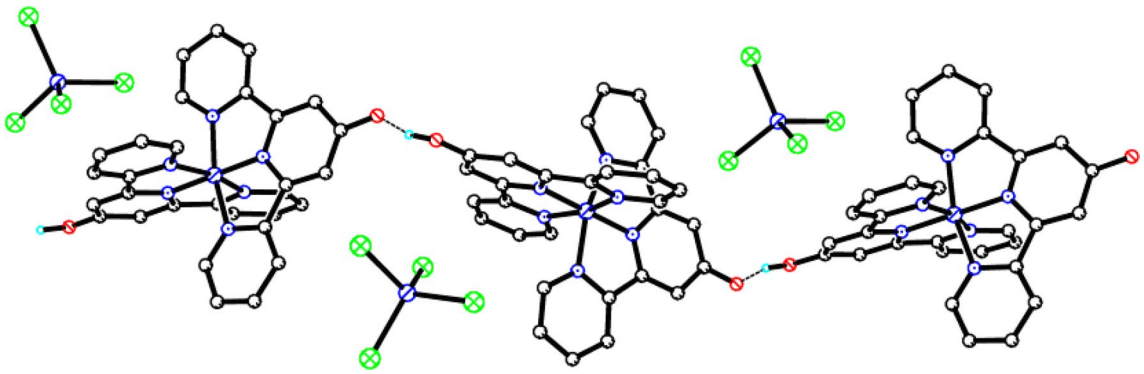

Fig. 4 Part of one chain of [Co(tpyOH)(tpyO)][$CoCl_4$]·H_2O (**2**) in b axis

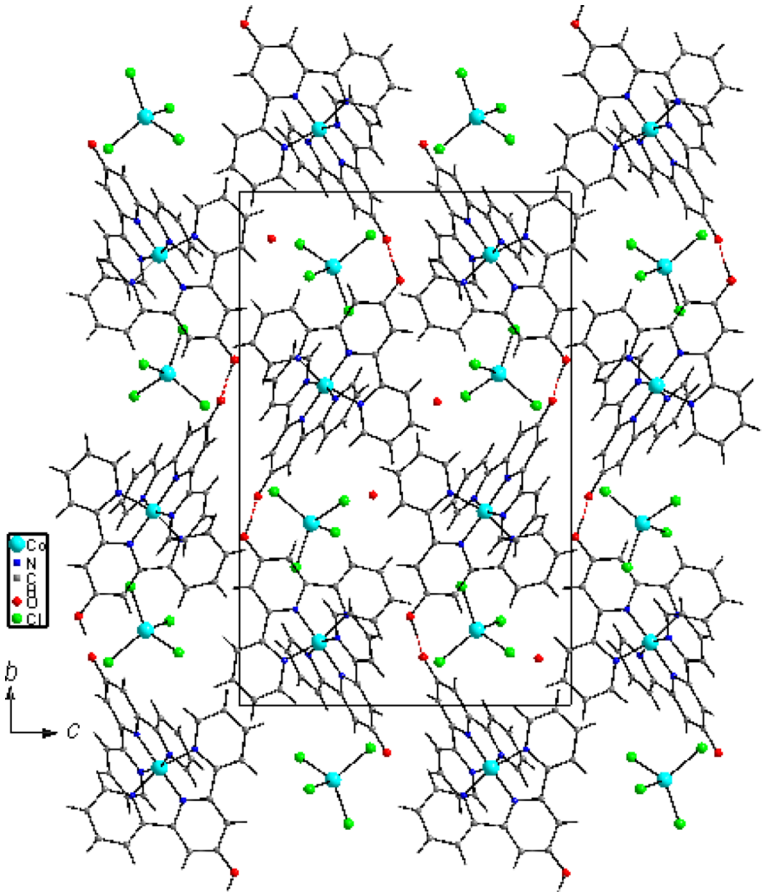

Fig. 5 Packing view of $[Co(tpyOH)(tpyO)][CoCl_4]\cdot H_2O$ (**2**) formed by hydrogen bonding interaction between cations separated by $CoCl_4^{2-}$

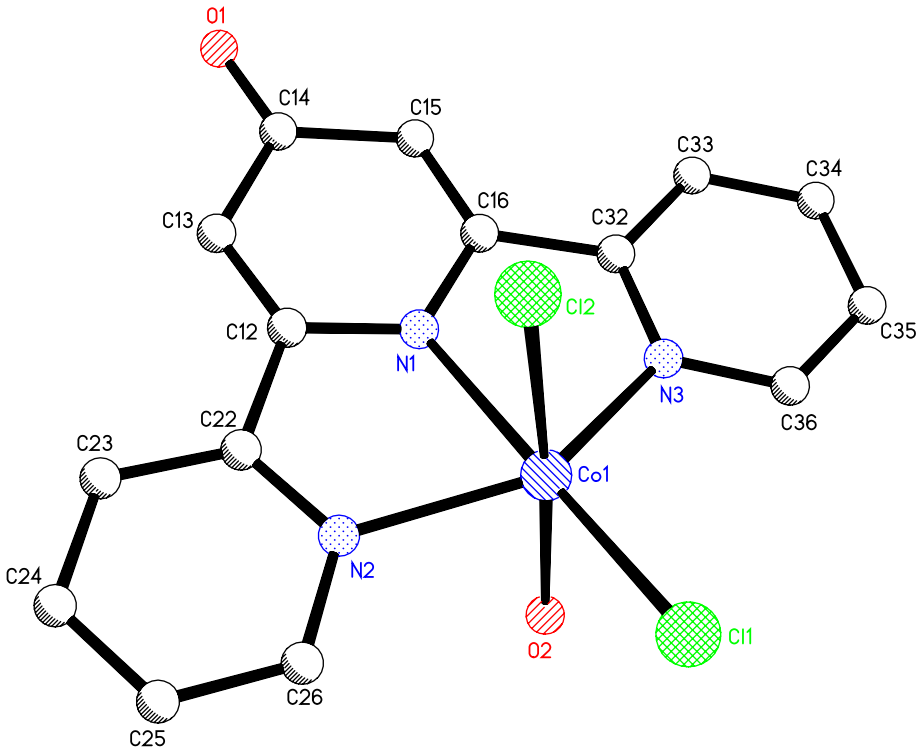

Fig. 6 ORTEP diagram of $[CoCl_2(H_2O)(tpyO)]\cdot H_2O$ (**3**). Selected bond distances (Å) and angles (°): Co1–N3 2.094(11), Co1–N2 2.103(11), Co1–O2 2.223(11), Co1–N1 2.250(10), Co1–Cl1 2.284(4), Co1–Cl2 2.454(4), N3–Co1–N2 139.9(4), N3–Co1–O2 86.8(4), N2–Co1–O2 83.0(4), N3–Co1–N1 71.3(4), N2–Co1–N1 70.9(4), O2–Co1-N1 94.6(4), N3–Co1–Cl1 109.4(3), N2–Co1–Cl1 108.9(3), O2–Co1–Cl1 87.9(3), N1–Co1–Cl1 177.4(3), N3–Co1–Cl2 95.0(3), N2–Co1–Cl2 93.2(4), O2–Co1–Cl2 175.8(3), N1–Co1–Cl2 82.4(3), Cl1–Co1–Cl2 95.06(16)

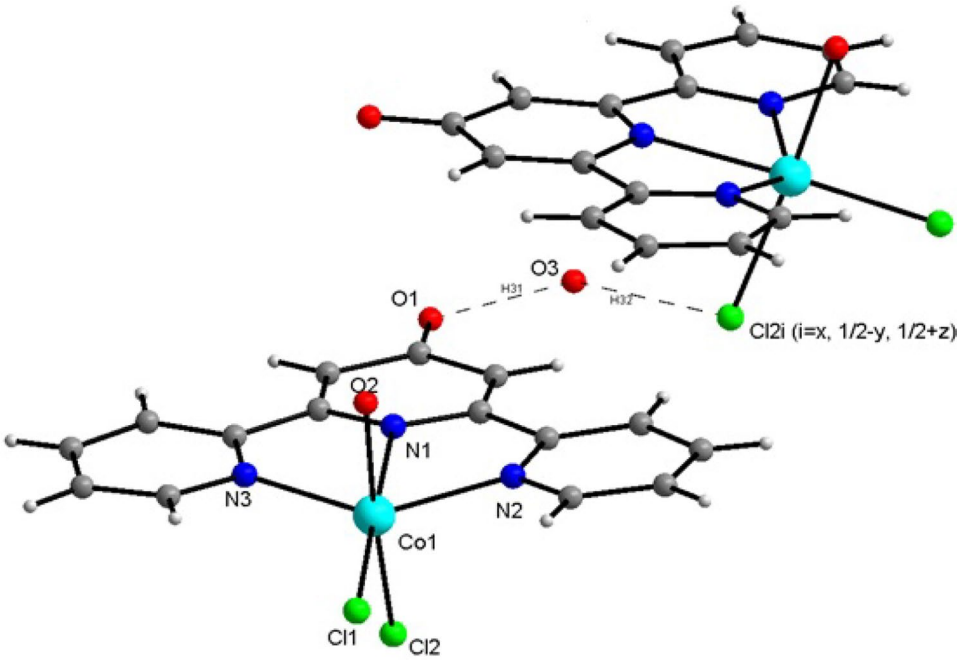

Fig. 7 The hydrogen bonding in complex $[CoCl_2(H_2O)(tpyOH)]\cdot H_2O$ (**3**)

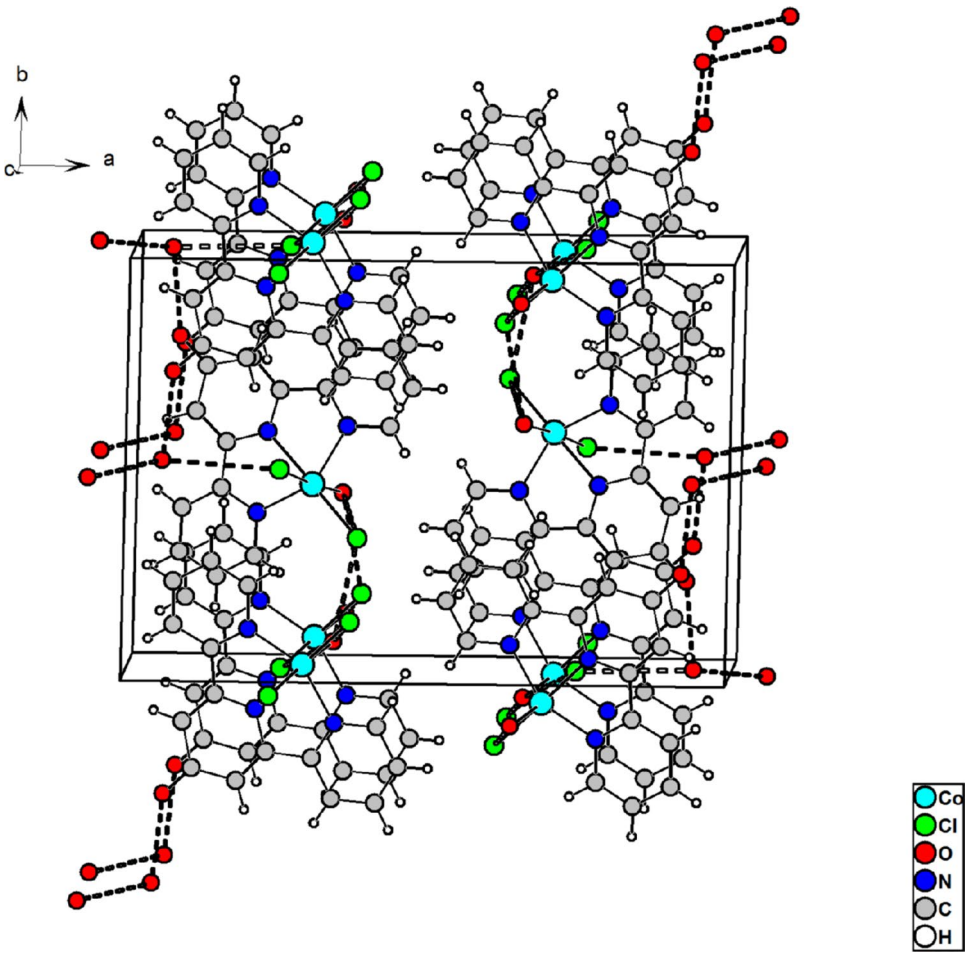

Fig. 8 Crystal packing of $[CoCl_2(H_2O)(tpyOH)]\cdot H_2O$ (**3**) in ab plane

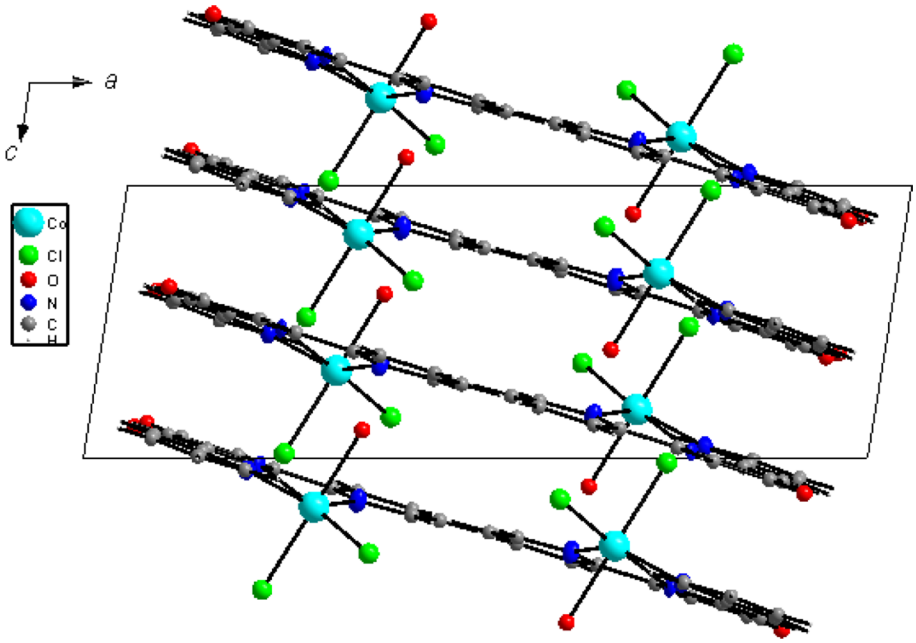

Fig. 9 Crystal packing of $[CoCl_2(H_2O)(tpyOH)]\cdot H_2O$ (**3**) along b axis

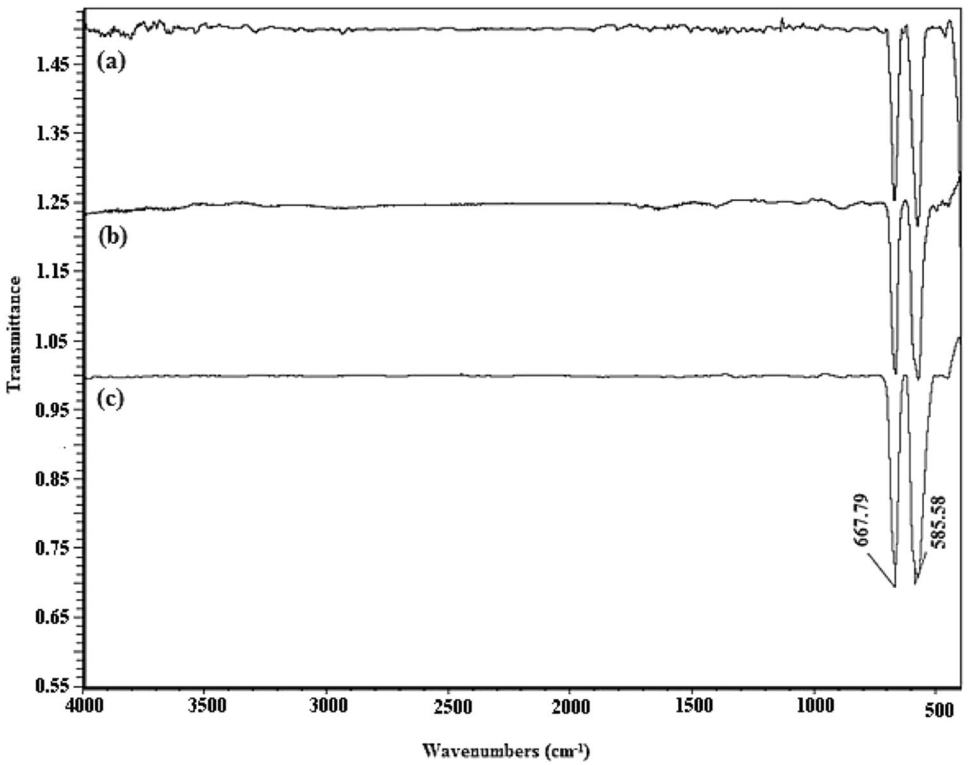

Fig. 10 The IR spectra of Co_3O_4 NPs derived from cobalt complexes (*a*) **1**, (*b*) **2** and (*c*) **3**

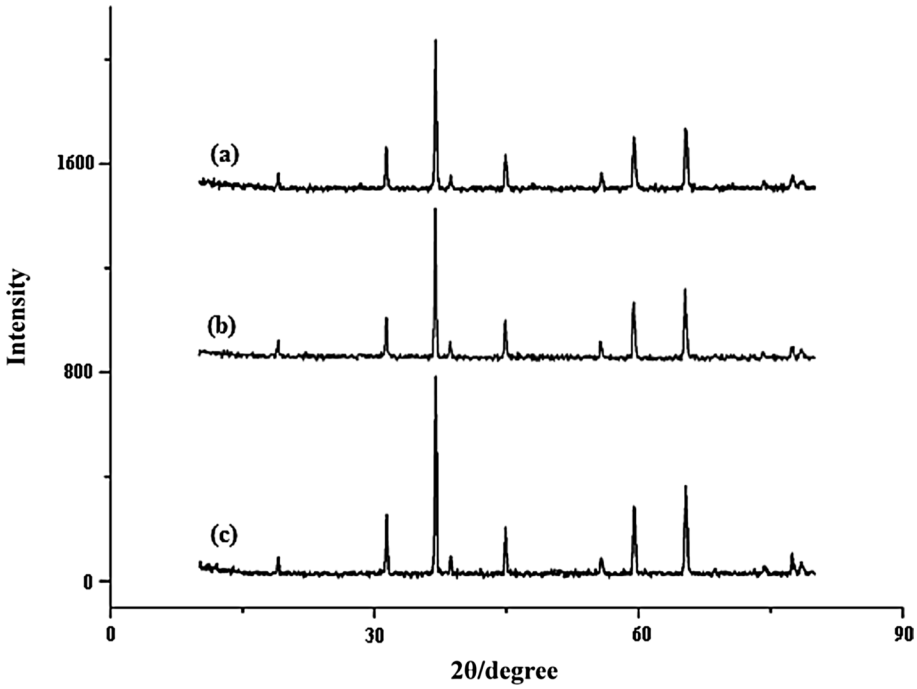

Fig. 11 XRD patterns for Co_3O_4 NPs obtained by calcination of the cobalt complexes (*a*) **1**, (*b*) **2** and (*c*) **3**

the successful synthesis of Co_3O_4 NPCs with the same structures. The FESEM images of the prepared Co_3O_4 NPs show the resulting Co_3O_4 NPCs from **1** to **3** have spherical morphology which contain agglomerated assembled spheres indicating a uniform homogeneity and good connectivity between the grains as shown in Fig. 13. On the other hand, the Co_3O_4 NPs obtained from **2** has the hexagonal shape in which the surfaces of the synthesized octahedral nanoparticles are almost smooth with no obvious defects (Fig. 13b). It seems that the structure of parent precursor complexes has influenced on the morphology of the final products. It can be seen that the well-shaped structures as well as the high crystalline nature of Co_3O_4 NPCs can be synthesized via the simple calcination of terpyridine complexes of cobalt. The mono terpyridine complexes results in the spherical structures; however, the bis-terpyridine complex **2** affords the hexagonal structure. The calcination of cobalt complex **2** led to the synthesis of Co_3O_4 NPCs with relatively fine particles of 32.25 nm compared to 35.11 and 33.17 nm for complexes **1** and **3**, respectively.

4.1 Thermal Properties of the Complexes

The thermal properties of the complexes were studied and the results are shown in Fig. 14. There are three major decomposition processes for $[Co^{II}Cl_2(tpyOH)]$ (**1**) as shown in Fig. 14a. The first loss is in the range of 107–125 °C and it concerns the loss of a hydration water molecule. The weight loss in this step is 3.74% (calc. 4.54%). The second step occurs in the temperature range of 360–469 °C with the weight loss of 19.17% (calc. 18.70%) which can be attributed to the loss of two coordinated chloride groups. The final decomposition process is from 535 to 614 °C with the weight loss of 66.17% (calc. 64.16%) which has been assigned to the decomposition of terpyridine ligand due to the loss of two and half pyridine moieties. On the other hand, the thermal stability of complex $[Co^{III}(tpyOH)(tpyO)][Co^{II}Cl_4]\cdot H_2O$ (**2**) indicates that thermal degradation occurred in four major steps (Fig. 14b). The first weight loss of 7.29% (calc. 6.51%) with the thermal stability up to 130 °C can be attributed to the loss of three coordinated water molecules. The second step is in the range of 140–340 °C with the weight loss of 6.26% (calc. 6.51%) which corresponds to the loss of one water molecule and one chloride moiety. The third weight loss is in the temperature range of 350–580 °C (16.39%) which seems to be associated with the loss of other three coordinated chloride moieties (calc. 14.74%). The final weight loss of 29.50% (calc. 27.98%) is in the range of 580–800 °C which might be due to loss of two pyridine and a hydroxyl group due to the decomposition of terpyridine ligands. The TGA curve of complex $[Co^{III}Cl_2(H_2O)(tpyO)]\cdot H_2O$ (**3**) shows three weight loss steps as shown in Fig. 14c. The first step includes the loss of coordination water molecule in the temperature range

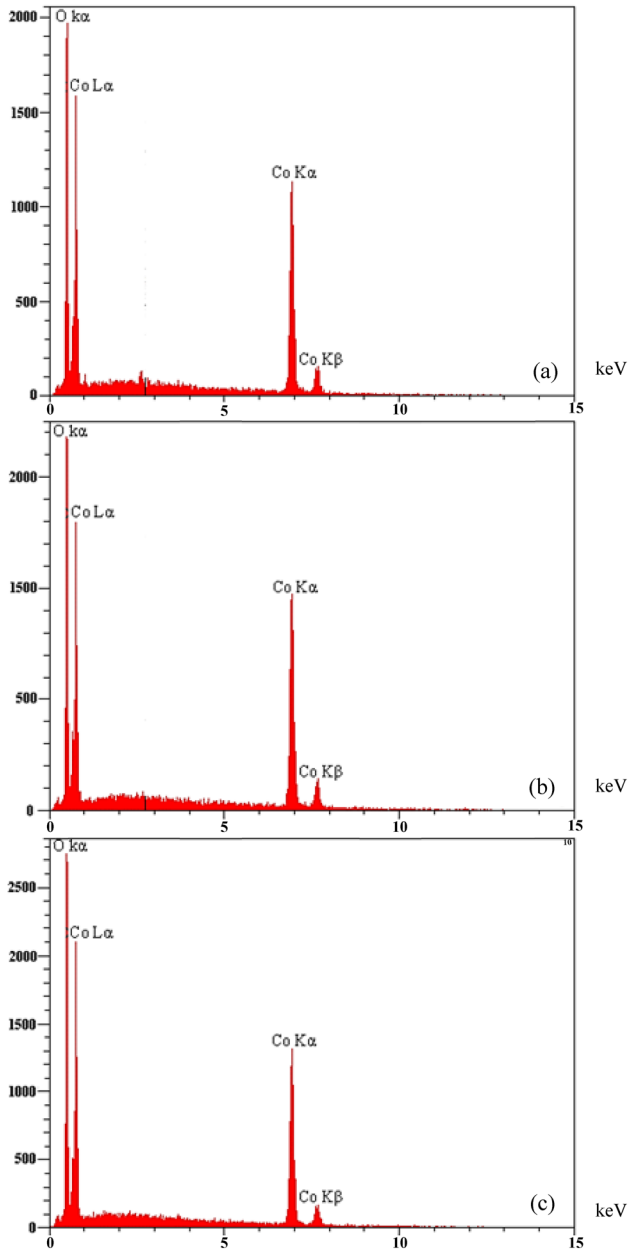

Fig. 12 EDX spectrum Co_3O_4 derived from cobalt complexes **a 1**, **b 2**, and **c 3**

of 340–371 °C with the weight loss of 5.86% (calc. 4.55%). The second weight loss (3.36%) is in the temperature range of 447–469 °C which is related to the release of half chloride moiety with the calculated amount of 4.68%. Finally, the weight loss of 78.68% occurs in the temperature range of 550–734 °C and it could refer to the loss of two and a half coordinated chloride moieties and tpyO moiety (calc. 78.73%). The thermal stabilities of the complexes indicate that the loss of free terpyridine ligand could not be observed in low temperatures due to the higher bond dissociation energies of the cobalt–nitrogen bond [30]. The thermal degradation of the complexes is slightly different from each other which may be due to their different structures. Therefore, metal complexes of terpyridine ligands exhibit good thermal stability which suggest them as the good candidate for a range of electronic device applications [49, 50].

5 Conclusion

The synthesis, characterization, including three single crystal structure determination of three new Co(II) and Co(III) complexes derived from 4′-hydroxy-2,2′:6′,2"-terpyridine by different routes have been described. It has been shown that solvent, temperature and reaction time are effective on the structures of the resulting complexes. In addition, 4′-hydroxy substituent plays a significant role in the structure of the complexes. The results could offer new strategy for design of supramolecular structures of cobalt using substituted terpyridine ligands which adopt several coordination modes. These complexes are important in catalysis, biological systems, photosensitizers and magnetism [9, 10, 51–53]. The thermal stabilities of the cobalt complexes indicate that the loss of free terpyridine ligand was not observed in low temperatures due to the higher bond dissociation energies of Co–N bond. The thermogravimetric analysis of complexes reveal the role of hydrogen bonding on the thermal stability of them. The results show the preparation of Co_3O_4 nanoparticles with hexagonal and spherical morphology from the terpyridine complexes of cobalt.

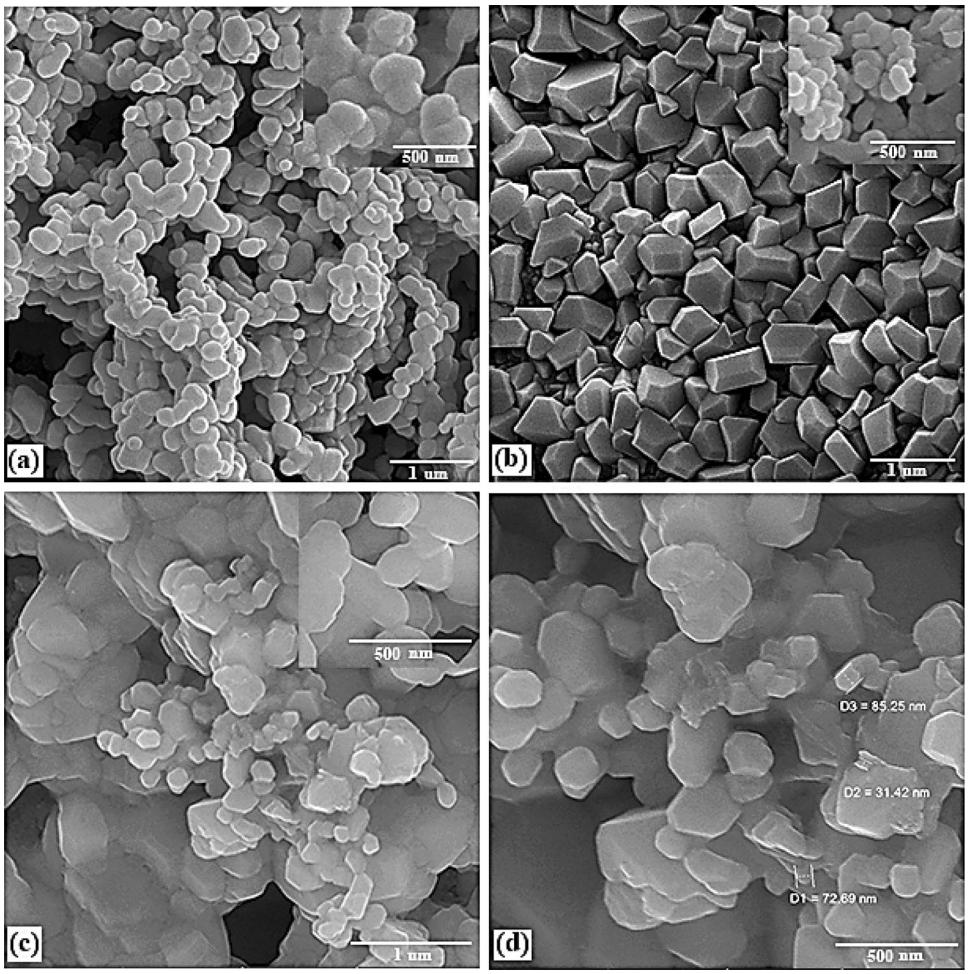

Fig. 13 FESEM images of the Co_3O_4 NPs derived from cobalt complexes (**1**) (**a**), (**2**) (**b**), (**3**) (**c**). Image **d** shows the particle sizes for (**c**)

6 Supplementary Material

CCDC 1434767, 1434769 and 1434768 contain the supplementary crystallographic data for **1, 2** and **3**, respectively. This data can be obtained free of charge via http://www.ccdc.cam.ac.uk/conts/retrieving.html, or from the Cambridge Crystallographic Data Centre, 12 Union Road, Cambridge CB2 1EZ, UK; fax: (+44) 1223 336 033; or e-mail: deposit@ ccdc.cam.ac.uk.

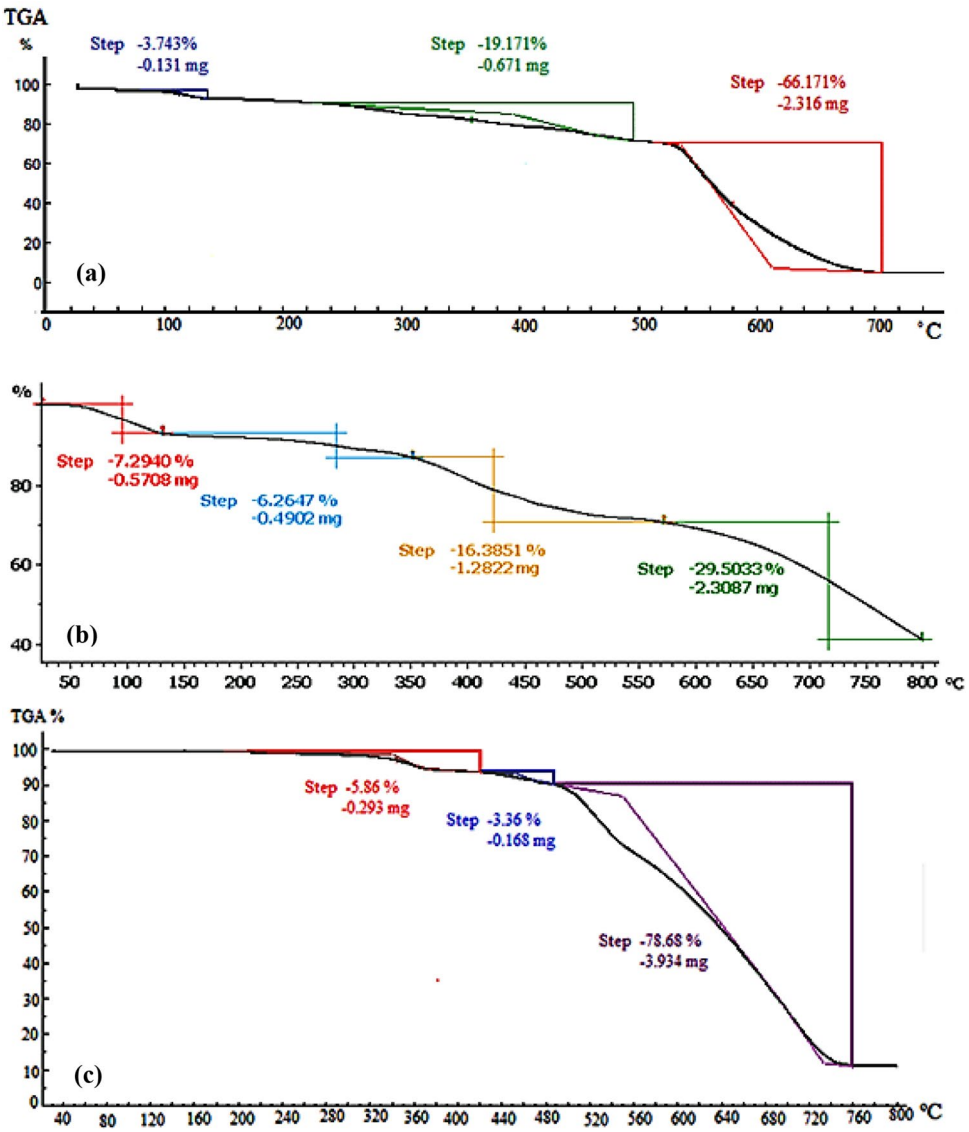

Fig. 14 TGA of $[CoCl_2(tpyOH)]$ **1** (**a**), $[Co(tpyOH)(tpyO)][CoCl_4]\cdot H_2O$ **2** (**b**), and, $[Co(tpyO)(H_2O)Cl_2]\cdot H_2O$ **3** (**c**)

Acknowledgements We would like to thank the Iran National Science Foundation (INSF) for financial support (Grant No. 93051215). We also thank the Science Research Council of K.N. Toosi University of Technology for financial support. We greatly appreciate Professor Jan Janczak for his helpful advice on X-ray crystallography.

References

1. G.T. Morgan, F.H. Burstall, J. Chem. Soc. **20**, 20 (1932)
2. R.A. Fallahpour, Synthesis **2003**, 155 (2003)
3. J. Wang, G.S. Hanan, Synlett. 8:1251 (2005)
4. M.N. Patel, H.N. Joshi, C.R. Patel, J. Organomet. Chem. **701**, 8 (2012)
5. F. Kröhnke, Synthesis **1976**:15 (1976)
6. R.-A. Fallahpour, E.C. Constable, J. Chem. Soc. Perkin Trans. **1**, 2263 (1997)
7. G. Zhang, J. Tan, Y.Z. Zhang, C. Ta, S. Sanchez, S.-Y. Cheng, J.A. Golen, A.L. Rheingold, Inorg. Chim. Acta **435**, 147 (2015)
8. E.C. Constable, C.E. Housecroft, V. Jullien, M. Neuburger, S. Schaffner, Inorg. Chem. Commun. **9**, 504 (2006)
9. Z. Naseri, A. Nemati Kharat, A. Banavand, A. Bakhoda, S. Foroutannejad, Polyhedron **33**, 396 (2012)
10. A.N. Kharat, A. Bakhoda, B.T. Jahromi, Polyhedron **30**, 2768 (2011)
11. R. Indumathy, M. Kanthimathi, T. Weyhermuller, B.U. Nair, Polyhedron **27**, 3443 (2008)
12. M. Chiper, M.A.R. Meier, J.M. Kranenburg, U.S. Schubert, Macromol. Chem. Phys. **208**, 679 (2007)
13. J.E. Beves, E.C. Constable, C.E. Housecroft, C.J. Kepert, D.J. Price, CrystEngComm **9**, 456 (2007)
14. J.E. Beves, E.C. Constable, C.E. Housecroft, M. Neuburger, S. Schaffner, CrystEngComm **10**, 344 (2008)
15. J.E. Beves, D.J. Bray, J.K. Clegg, E.C. Constable, C.E. Housecroft, K.A. Jolliffe, C.J. Kepert, L.F. Lindoy, M. Neuburger, D.J. Price, S. Schaffner, F. Schaper, Inorg. Chim. Acta **361**, 2582 (2008)
16. U.S. Schubert, C. Eschbaumer, O. Hien, P.R. Andres, Terahedron Lett. **42**, 4705 (2001)

17. E.C. Constable, E.L. Dunphy, C.E. Housecroft, M. Neuburger, S. Schaffner, F. Schaper, S.R. Batten, Dalton Trans. **38**, 4323 (2007)
18. F. Yuan, S.-S. Shen, H.-M. Hu, R. An, X. Wang, Z. Chang, G. Xue, Inorg. Chim. Acta **430**, 17 (2015)
19. A.S. Abd-El-Aziz, J.L. Pilfold, B.Z. Momeni, A.J. Proud, J.K. Pearson, Polym. Chem. **5**, 3453 (2014)
20. B.Z. Momeni, S. Heydari, Polyhedron **97**, 94 (2015)
21. J. McMurtrie, I. Dance, CrystEngComm **7**, 230 (2005)
22. J. McMurtrie, I. Dance, CrystEngComm **12**, 2700 (2010)
23. Y. Wang, G. Chen, L. Han, J. Pei, J. Solid State Chem **206**, 251 (2013)
24. V. Fernández-Moreira, F.L. Thorp-Greenwood, R.J. Arthur, B.M. Kariuki, R.L. Jenkins, M.P. Coogan, Dalton Trans **39**, 7493 (2010)
25. K.A. Maghacut, A.B. Wood, W.J. Boyko, T.J. Dudley, J.J. Paul, Polyhedron **67**, 329 (2014)
26. J.R. Jeitler, M.M. Turnbull, Acta Cryst **E61**, m1846 (2005)
27. A. Galet, A.B. Gaspar, M.C. Muňoz, J.A. Real, Inorg. Chem. **45**, 4413 (2006)
28. P. Nielsen, H. Toftlund, A.D. Bond, J.F. Boas, J.R. Pilbrow, G.R. Hanson, C. Noble, M.J. Riley, S.M. Neville, B. Moubaraki, K.S. Murray, Inorg. Chem. **48**, 7033 (2009)
29. A.B. Gaspar, M.C. Muňoz, V. Niel, J.A. Real, Inorg. Chem. **40**, 9 (2001)
30. S. Hayami, Y. Komatsu, T. Shimizu, H. Kamihata, Y.H. Lee, Coord. Chem. Rev. **255**, 1981 (2011)
31. T. Wieprecht, J. Xia, U. Heinz, J. Dannacher, G. Schlingloff, J. Mol. Catal. A **203**, 113 (2003)
32. V. Raman, S. Suresh, P.A. Savarimuthu, T. Raman, A.M. Tsatsakis, K.S. Golokhvast, V.K. Vadivel, Exp Ther. Med. **11**, 553 (2016)
33. S. Gopinath, K. Sivakumar, B. Karthikeyen, C. Ragupathi, R. Sundaram, Phys. E **81**, 66 (2016)
34. B. Varghese, T.C. Hoong, Z. Yanwu, M.V. Reddy, B.V.R. Chowdari, A.T.S. Wee, T.B.C. Vincent, C.T. Lim, C.-H. Sow, Adv. Funct. Mater. **17**, 1932 (2007)
35. D.D.M. Prabaharan, K. Sadaiyandi, M. Mahendran, S. Sagadevan, Appl. Phys. A **123**, 264 (2017)
36. V.R. Shinde, S.B. Mahadik, T.P. Gujar, C.D. Lokhande, Appl. Surf. Sci. **252**, 7487 (2006)
37. M. Pudukudy, Z. Yaakob, Chem. Pap. **68**, 1087 (2014)
38. L. Sun, H. Li, L. Ren, C. Hu, Solid State Sci. **11**, 108 (2009)
39. H. Wang, L. Zhang, X. Tan, C.M.B. Holt, B. Zahiri, B.C. Olsen, D. Mitlin, J. Phys. Chem. C **115**, 17599 (2011)
40. H. Sadeghzadeh, A. Morsali, V.T. Yilmaz, O. Büyükgüngör, Mater. Lett. **64**, 810 (2010)
41. A. Dehno Khalaji, M. Nikookar, K. Fejfarova, M. Dusek, J. Mol. Struct. **107**, 6 (2014)
42. M. Salavati-Niasari, A. Khansari, C. R. Chim **17**, 352 (2014)
43. A. Mehrani, A. Morsali, J. Mol. Struct. **1074**, 596 (2014)
44. L. Dolatyari, P. Seddigi, A. Ramazani, M.G. Amiri, J. Struct. Chem. **54**, 571 (2013)
45. E.C. Constable, M.D. Ward, J. Chem. Soc. Dalton Trans.4:1405 (1990)
46. G.M. Sheldrick, *Bruker Analytical X-Ray-Division*, Bruker Corp., Madison (2012)
47. G.M. Sheldrick, SHELXL-2014 Program, (Sheldrick, 2014) for structure refinement. Acta Cryst. C **71**, 3 (2015)
48. R. Jenkins, R.L. Snyder, *Introduction to X-ray powder diffractometry Chemical Analysis*: vol. 138 (Wiley, New York, 1996),
49. S.-H. Hwang, C.N. Moorefield, P. Wang, J.-Y. Kim, S.-W. Lee, G.R. Newkome, Inorg. Chim. Acta **360**, 1780 (2007)
50. J. Kuwabara, T. Namekawa, M. Haga, T. Kanbara, Dalton Trans. **42**, 44 (2012)
51. S. Aroua, T.K. Todorova, P. Hommes, L.-M. Chamoreau, H.-U. Reissig, V. Mougel, M. Fontecave, Inorg. Chem. **56**, 373 (2017)
52. H. Hofmeier, U. Schubert, Chem. Soc. Rev. **33**, 373 (2004)
53. B. Xu, B. Liu, H.-M. Hu, Y. Cheng, Z. Chang, G. Xue, Polyhedron **96**, 88 (2015)